

Using bioinformatics and systems genetics to dissect HDL-cholesterol genetics in an MRL/MpJ × SM/J intercross[§]

Magalie S. Leduc,^{1,*†} Rachael Hageman Blair,^{**§} Ricardo A. Verdugo,^{*} Shirng-Wern Tsaih,^{**} Kenneth Walsh,^{*} Gary A. Churchill,^{*} and Beverly Paigen^{*}

The Jackson Laboratory,^{*} Bar Harbor, ME; Texas Biomedical Research Institute,[†] San Antonio, TX; State University of New York at Buffalo,[§] Buffalo, NY; and Human and Molecular Genetics Center,^{**} Medical College of Wisconsin, Milwaukee, WI

Abstract A higher incidence of coronary artery disease is associated with a lower level of HDL-cholesterol. We searched for genetic loci influencing HDL-cholesterol in F2 mice from a cross between MRL/MpJ and SM/J mice. Quantitative trait loci (QTL) mapping revealed one significant HDL QTL (*Apoa2* locus), four suggestive QTL on chromosomes 10, 11, 13, and 18 and four additional QTL on chromosomes 1 proximal, 3, 4, and 7 after adjusting HDL for the strong *Apoa2* locus. A novel nonsynonymous polymorphism supports *Lipg* as the QTL gene for the chromosome 18 QTL, and a difference in *Abca1* expression in liver tissue supports it as the QTL gene for the chromosome 4 QTL. Using weighted gene co-expression network analysis, we identified a module that after adjustment for *Apoa2*, correlated with HDL, was genetically determined by a QTL on chromosome 11, and overlapped with the HDL QTL. A combination of bioinformatics tools and systems genetics helped identify several candidate genes for both the chromosome 11 HDL and module QTL based on differential expression between the parental strains, *cis* regulation of expression, and causality modeling. **■** We conclude that integrating systems genetics to a more-traditional genetics approach improves the power of complex trait gene identification.—Leduc, M. S., R. H. Blair, R. A. Verdugo, S-W. Tsaih, K. Walsh, G. A. Churchill, and B. Paigen. Using bioinformatics and systems genetics to dissect HDL-cholesterol genetics in an MRL/MpJ × SM/J intercross. *J. Lipid Res.* 2012. 53: 1163–1175.

Supplementary key words high-density lipoprotein cholesterol • gene suppression • genomics

This study was funded by National Institutes of Health Grants HL-077796 and HL-081162 (B.P.) and GM-070683 (G.A.C.), American Heart Association post-doctoral Fellowship 09POST2040006 (M.S.L.), National Heart, Lung, and Blood Institute NSRA Fellowship 1F32HL095240 (R.H.B.), and National Cancer Institute Core Grant CA034196 to The Jackson Laboratory. Its contents are solely the responsibility of the authors and do not necessarily represent the official views of the National Institutes of Health or other granting agencies.

Manuscript received 28 February 2012 and in revised form 10 April 2012.

Published, JLR Papers in Press, April 11, 2012
DOI 10.1194/jlr.M025833

Copyright © 2012 by the American Society for Biochemistry and Molecular Biology, Inc.

This article is available online at <http://www.jlr.org>

A higher incidence of coronary artery disease (CAD) is associated with a lower level of HDL-cholesterol (1, 2), which is determined by multiple environmental and genetic factors. In the past few years, new therapeutic approaches have focused on finding ways to increase HDL (3, 4). To date, however, only a few environmental interventions, such as diet and exercise, have been successful in raising HDL level (5), whereas drug therapy development is still ongoing and has targeted only a limited number of proteins such as CETP (3, 4). In the search for a potential drug target to raise HDL and decrease CAD, the identification of new genes involved in HDL determination is essential.

The genetic basis of HDL-cholesterol variation has been widely studied in various animal models. In humans, recent genome-wide association studies (GWAS) have identified known HDL genes such as *LIPG* and *CETP* in addition to new genes such as *GALNT2* (6). These known genes, however, explain only a small proportion of the total variation, indicating that additional genes are yet to be discovered. Mouse models are a powerful strategy for identifying such genes. A large overlap exists among species for quantitative trait loci (QTL) and genes involved in lipid metabolism (7). Many study methodologies are similar between human and mouse, but mouse studies offer advantages by capitalizing on genomics tools that are not available and practical for studies of human populations. To date, our laboratory and those of others have identified over 35 mouse HDL QTL (as reviewed in Wang et al., Refs. 7, 8). In addition, we and others have developed bioinformatics tools to narrow the QTL interval to just a few candidate genes (9, 10). Application of these tools has led to the discovery of single genes underlying QTL for HDL and

Abbreviations: CAD, coronary artery disease; CGD, Center for Genome Dynamic; eQTL, expression QTL; LOD, logarithm of the odds; QTL, quantitative trait loci; WGCNA, weighted gene co-expression network analysis.

[†]To whom correspondence should be addressed.

e-mail: mleduc@txbiomedgenetics.org

[§]The online version of this article (available at <http://www.jlr.org>) contains supplementary data in the form of two figures and six tables.

other complex traits. However, the addition of systems genetic approaches allows for identification of a group of genes that influences a complex trait as a group, not individually, and that usually represents a functional and biological process that influences the trait (11, 12).

We recently reported the results of the MRL/MpJxSM/J (MRLxSM) cross for triglycerides (13) and showed how our bioinformatics tool, in addition to genome-wide expression analysis and causality modeling, represents a powerful strategy for identifying candidate genes for QTL. Here, we report the results of our QTL analysis between inbred mouse strains MRL and SM for HDL-cholesterol level. We identified several HDL QTL, and we applied our bioinformatics tool to add molecular evidence for the known genes *Abca1* and *Lipg* and narrow the additional QTL to just a few candidate genes based either on the presence of nonsynonymous coding polymorphisms segregating between the parental strains or expression differences between the parental strains. In addition, we took advantage of the availability of the expression level of the transcripts in the F2 mice to 1) improve the QTL gene identification by leveraging expression QTL (eQTL) and correlation, and 2) apply the weighted gene co-expression network analysis (WGCNA). WGCNA allowed us to identify gene modules of tightly connected and correlated genes that are themselves correlated with HDL-cholesterol (11, 12). The identification of the underlying genetics of these modules adds a new dimension in the identification of genes regulating HDL-cholesterol at the genome-wide level and helped identify several candidate genes for the chromosome 11 HDL QTL through the combined use of bioinformatics and systems genetics.

MATERIALS AND METHODS

Mice

MRL/MpJ (MRL) and SM/J (SM) mice were obtained from the Jackson Laboratory (Bar Harbor, ME) and mated to produce F1 mice (by intercrossing MRL females with SM males) and reciprocal F1 (RF1) mice (by intercrossing SM females with MRL males). Two hundred eighty-two F2 mice were produced by brother-sister mating of F1 mice. All mice were bred and housed in a climate-controlled pathogen-free facility at the Jackson Laboratory with a 12:12 h light-dark cycle. F1, RF1, and F2 males and females were weaned at 21 days and fed chow diet (LabDiet® 5K52, PMI Nutritional International; Bentwood, MO). Mice were euthanized at 13 weeks of age, and livers were collected as previously described (14). All experiments were approved by the Jackson Laboratory Animal Care and Use Committee.

HDL measurements

Blood samples were obtained from 8-week-old mice fasted for 4 h prior to retro-orbital bleeding. Blood was collected with EDTA, and plasma was isolated by centrifugation within 2 h of the bleed. The serum was frozen at -20°C for 1 week until measured. HDL-cholesterol was measured using a synchron CX Delta System (Beckman Coulter; Fullerton, CA). The chemical method first allows for the separation of HDL particles from non-HDL particles using detergents. The HDL particles are then solubilized, and the cholesterol reacts to the cholesterol esterase, cholesterol oxidase, and chromogens. The change in absorbance, measured at 560 nm, represents the H_2O_2 released in these reactions, which is proportionate to the amount of HDL in the sample. The method

has been validated in-house for use in mice. The system is calibrated prior to weekly measurements, and controls are run on a weekly basis.

Genotyping

Mice were tail-tipped at 10 days of age. The DNA extraction and genotyping has previously been described (14). Briefly, DNA was isolated using phenol-chloroform and genotyped for 259 markers using the Illumina platform and custom sequencing. Genetic and physical positions were determined using the newly calculated map available on the Center for Genome Dynamic (CGD) website hosted at the Jackson Laboratory, which gather numerous analytical tools and large-scale datasets used to analyze the mammalian genome (15).

Microarray

Microarrays were processed as described previously (13, 14) using Mouse Gene 1.0 ST microarray (1M) (Affymetrix; Santa Clara, CA). RNA extracted from F2 mouse livers was hybridized onto the array. The R language/environment version 2.7.2 for data analyses was used to process the results, and affy V1.20.0 and preprocessCore V1.6 packages from Bioconductor were used to perform quality control and quantile normalization (16). The transcript analysis was performed with a custom CDF file (17) for Ensembl transcripts (ENST package V.11, 37,264 probesets) from the BrainArray (University of Michigan) website. Redundant probesets in the CDF file were removed, which produced a dataset with 34,406 probesets (or transcripts) for following analyses. Transcript levels from the microarray results were used to assess the difference in expression between the parental strains at each candidate gene locus, and for expression QTL and correlation in the F2 mice as described below. Microarrays are available at the Gene Expression Omnibus (GEO accession: GSE25322).

QTL analysis

Linkage analysis was performed using R/ql for HDL and all 34,406 transcripts in 282 F2 mice (v1.09-43) (18). A three-step analysis was applied. First, QTL analysis was investigated by adding sex as an additive covariate. Second, sex was added as an interactive covariate. The difference between the interactive and additive models is a test for sex-specific QTL: if the logarithm of the odds (LOD) difference between both models is higher than 2, it indicates that the QTL may be specific to males or females. Third, epistatic effects or interacting QTL were examined using the pairscan function. In addition, if the presence of two QTL on the same chromosome was suspected, two models were compared: a model with one QTL against a model with both QTL. If the LOD difference between both models was higher than 2, it indicated the presence of two QTL on the same chromosome. On chromosome 1, a high LOD score was found due to the *Apoa2* locus. Therefore, a similar QTL analysis for each model was performed after adding the closest single nucleotide polymorphism (SNP) to *Apoa2* (rs13476248) as a covariate. We renamed the phenotype HDL^{*Apoa2*}, HDL level adjusted for the *Apoa2* locus. The Bayesian estimation of the 95% confidence interval was used. All suggestive and significant QTL were included in a combined multi-locus model, and the proportion of the variation explained by each QTL was determined through regression analysis. For the transcripts, QTL analysis was performed using the Haley Knott method with a 2 cM interval and sex as an additive covariate. Any gene that had a transcript with a suggestive LOD score within 20 cM of the gene location was considered *cis*-regulated. Finally, QTL analysis in males and females was performed separately, on HDL (with and without adjustment for the *Apoa2* locus) and on the transcripts. Thresholds for significant ($P < 0.05$) and suggestive ($P < 0.63$) LOD scores were based on 1,000 permutations of the observed data for the autosomes, 17,940

permutations for the X chromosome for HDL, and 10,000 permutations for the transcripts (19). The genotypes and phenotypes are publically available at the CGD website.

Bioinformatic approach

Our bioinformatic approach has previously been described (9, 10). Briefly, the list of genes located under each QTL was downloaded from BioMart. First, using the CGD imputed SNP database, each gene was searched for a nonsynonymous coding polymorphism that segregated between MRL and SM that was characterized as being “damaging” using SIFT (20). Second, a search was made for genes that showed evidence of a differential expression between MRL and SM and for which the expression was 1) *cis*-regulated, 2) significantly different between MRL and SM in males or females, and 3) correlated with HDL^{Apoa2}. Any genes that were located under a QTL of interest (phenotype and module) and were based on differential gene expression were subject to causal analysis using conditional genome scans as described previously (13, 21, 22). In this analysis, we use the conditional LOD score as a formal measure of conditional independence. Specifically, for a phenotype, Y1, with a QTL, Q, a gene expression trait, T1, is used as a covariate in the QTL mapping. A decrease in the LOD score for a QTL of interest below the suggestive level after conditioning is evidence of a causal relationship.

Weighted gene co-expression network

WGCNA was performed on expression results from the liver from the 282 F2 mice using the WGCNA package implemented in R (12). If a gene had more than one probe set, the transcript with the highest connectivity (K_{int}) was selected, resulting in 22,120 transcripts representing unique genes. Due to the high number of transcripts, a blockwise approach was implemented in the WGCNA package where the genes were first divided into sets of genes. Within each block, pairwise correlations were calculated and the adjacency matrix was calculated by raising each pairwise correlation to the power of the soft threshold β . To reach a minimum power of 0.85, β was determined to be equal to 2 in the F2 population and males only, and 3 in females only. The weighted topological overlap matrix was then calculated and cut using the dynamic cutting tree to identify modules of highly correlated transcripts. The maximum number of transcripts was set to 2,000 per block, the minimum number of genes per module was set to 100, and the minimum height for merging modules was set to 0.2. The module eigengenes derived from the program were tested for correlation with HDL and HDL^{Apoa2} (23). Gene ontology was used to identify common functional pathways between genes in the significant modules.

Statistical analysis

Parental strains, F1, RF1, and F2 mice were compared with ANOVA for females and males separately (JMP 7.0; The SAS institute, Cary, NC). The data were transformed using a Van Der Waerden normal score (24). Correlation between the transcript level and the phenotype (HDL^{Apoa2}) was calculated using Pearson correlation in R.

RESULTS

HDL cholesterol characteristics of the parental strains, F1, RF1, and F2 mice

Means and standard error of HDL are summarized in **Table 1**. MRL mice had statistically higher HDL compared with SM, F1, RF1, and F2 mice in males and females. SM mice had statistically lower HDL compared with F1, RF1, and F2 mice in males and females. No difference was observed between the two populations of F1 mice (F1 and RF1), indicating that levels of HDL in this intercross

TABLE 1. HDL level in the parental strains, F1s, RF1s, and F2s

Mice	N	HDL-cholesterol
Male		
MRL	10	162 ± 5.3
SM	15	86 ± 1.8 ^a
(MRL×SM) F1	33	107 ± 1.7 ^{a,b}
(SM×MRL) F1	14	117 ± 1.6 ^{a,b}
(MRL×SM) F2	147	117 ± 1.3 ^{a,b,c}
Female		
MRL	10	112 ± 2.4
SM	14	57 ± 1.8 ^a
(MRL×SM) F1	27	79 ± 2.1 ^{a,b}
(SM×MRL) F1	20	80 ± 1.6 ^{a,b}
(MRL×SM) F2	135	80 ± 1.2 ^{a,b}

^a $P < 0.01$ versus MRL.

^b $P < 0.01$ versus SM.

^c $P < 0.01$ versus (MRL × SM) F1.

were not affected by an imprinted gene, a gene located on the X chromosome, or mitochondrial DNA.

Identification of genomic loci underlying HDL levels in the F2 mice

Figure 1 and supplementary Fig. I represent the genome-wide scans for HDL, and **Table 2** indicates positions of the QTL with a 95% confidence interval, LOD scores for the relevant model, the closest marker, the high allele strain at the locus, and the mode of inheritance. The allele effect plots at each QTL are provided in supplementary Fig. II. We identified four main-effect HDL QTL: one each on Chr1@81.8cM (*Hdlq15*), Chr10@30.9cM, Chr11@42.7cM (*Hdlq81*), and Chr18@40.3cM (Fig. 1A and Table 2). For the QTL on chromosomes 1, 11, and 18, mice homozygous for the MRL allele had higher HDL levels, in an additive manner, compared with mice homozygous for the SM allele (see supplementary Fig. II). On chromosome 10, mice homozygous for the MRL and SM alleles did not differ in HDL, but heterozygous mice had higher HDL than did MRL and SM homozygous mice (see supplementary Fig. II). We identified a female-specific QTL on Chr13@33.6cM (see supplementary Figs. I, II): females showed a free model of inheritance, with MRL and SM homozygous females carrying higher HDL compared with heterozygous females; males showed no such pattern. We performed pairscan analysis and identified one QTL interacting with the chromosome 1 locus (*Hdlq15*) on Chr7@58.2cM (*Hdlq80*). MRL mice had higher HDL compared with SM mice, but the mode of inheritance was dependent on the genotype of the chromosome 1 locus (*Hdlq15*): we observed a dominant, recessive, or additive mode of inheritance of the MRL allele if the mice were homozygous for the MRL allele, homozygous for the SM allele, or heterozygous, respectively (see supplementary Fig. II). The highest LOD score was observed for Chr1@81.8cM, corresponding to the apoA-II (*Apoa2*) locus. Wang et al. (25) previously identified *Apoa2* as the QTL gene for several crosses (10), and we expected an HDL QTL in this region based on the MRL and SM haplotype. Because the unusually strong effect of the *Apoa2* locus on HDL level in this cross may mask other QTL, we adjusted the HDL level for the *Apoa2* locus and

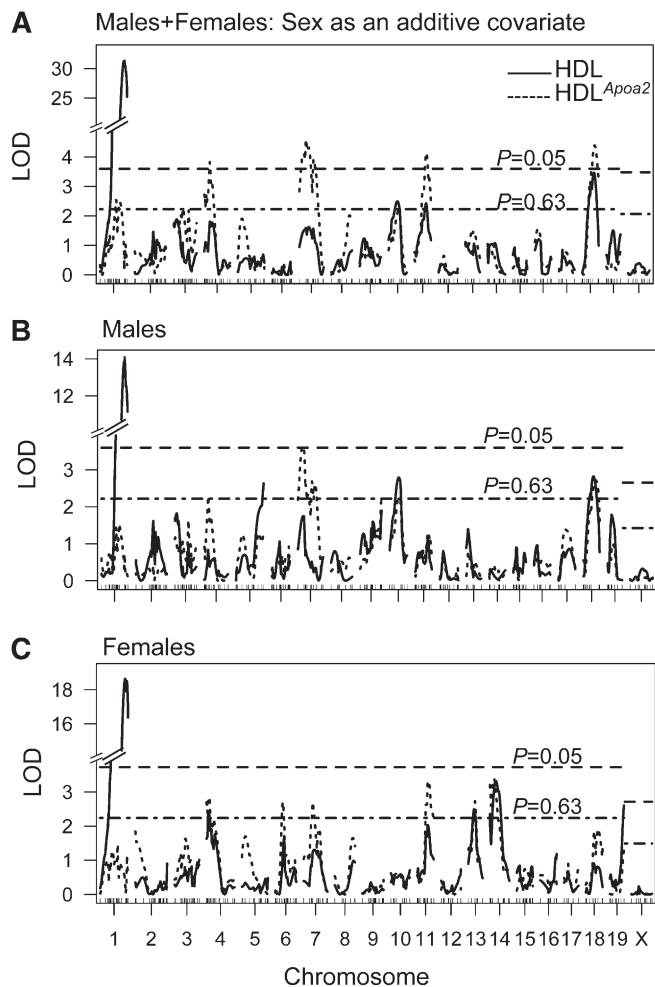


Fig. 1. Genome-wide scan for HDL level in 282 F2 mice. Analysis was performed with sex as an additive covariate on HDL level (A) (solid line). Because of the high LOD score on chromosome 1, we adjusted the HDL for the chromosome 1 (*Apoa2*) locus by adding the closest SNP to *Apoa2* (rs13476248) as a covariate (dotted line). The results using sex as an interactive covariate are provided in supplementary Fig. 1. QTL analysis was also performed in males (n = 147) (B) and females (n = 135) (C) separately for HDL (solid line) and HDL adjusted for the *Apoa2* locus (dotted line). For each model, data were permuted 1,000 times to determine the genome-wide level of significance. The threshold of significance for chromosome X was determined with 17,940 permutations. The dashed line represents the threshold of ($P = 0.05$) and the dot-dashed line represents the threshold for suggestive QTL ($P = 0.63$).

renamed this phenotype HDL^{*Apoa2*}. We used the closest marker (rs13476248), located at 79.3 cM, as an additive covariate in addition to sex (Fig. 1). We identified four additional QTL on Chr1@53.6cM, Chr3@23cM, Chr4@20cM (*Hdlq78*), and Chr7@31.1cM (*Hdlq79*). The chromosome 11 and chromosome 18 loci (*Hdlq81* and *Hdlq82*) are located close to the previously identified HDL QTL (within 2 cM) and are likely to be the same QTL. Two QTL found in the first analysis before conditioning on *Apoa2* were not detected in this analysis: the female-specific QTL on chromosome 13 and the QTL on chromosome 10. We did not identify any QTL interaction because of the low number of mice with each genotype combination (*Apoa2* combined with two interactive QTL). We also suspected two QTL on chromosome 7,

but could not confirm this assumption ($\Delta\text{LOD} < 2$). We also performed QTL analysis in males and females separately (Fig. 1B, C) and, except for the chromosome 7 QTL, were able to confirm all significant QTL in at least one sex. The original peak at 31.1 cM was shifted to 22.1 cM in females and to 37.9 cM in males (Table 2 and Fig. 1), indicating that multiple sex-specific QTL may be present in this region of chromosome 7. The low resolution of an F2 cross does not allow the separation and precise identification of these QTL. Additional suggestive QTL were identified in the sex-specific analysis but were not pursued, due to the low LOD score and low number of mice in this type of analysis. Overall, in the combined sex analysis, we were able to explain 63.7% of the variation in HDL: sex explained 47.3% of the variation, and genetics explained 16.4% (Table 3). Because of the large sex effect, we investigated males and females separately; the proportion of genetic variation explained by the QTL was increased to 49.9% and 59.5% for HDL in males and females, respectively (Table 3).

Genomic dissection of the HDL QTL based on bioinformatics

We searched for candidate genes located under each significant QTL on chromosomes 4, 7, 11, and 18 that either 1) carried a nonsynonymous coding polymorphism segregating between MRL and SM that was predicted to be damaging (structural or functional molecular evidence), or 2) exhibited expression that was significantly different between MRL and SM, that was *cis*-regulated, and that correlated with HDL^{*Apoa2*} (expression molecular evidence) in males and females. None of the QTL found in the entire 282 F2 cohort were also found at the significance level in males or females separately (Fig. 1). Therefore, the search was based on the entire cohort of 282 F2 mice. The list of candidate genes for each QTL is indicated in supplementary Table I. Based on these bioinformatic data, we identified 27, 112, 87, and 21 candidate genes from 449, 1,502, 744, and 198 genes located under the QTL on chromosomes 4, 7, 11, and 18, respectively (Fig. 2 and supplementary Table I). Additionally, for each gene showing an expression difference, we performed conditional linkage to estimate whether the expression was likely to be responsible for the QTL. Based on causality only, we reduced the number of candidate genes to 7, 3, 25, and 1 for chromosomes 4, 7, 11, and 18, respectively (Fig. 2 and supplementary Table II). While none of the genes located under the HDL QTL on chromosomes 7 and 11 were known HDL genes, two of the QTL on chromosomes 4 and 18 harbor well-known HDL genes: *Abca1* and *Lipg*, respectively.

Abca1 has been identified as the QTL gene in four other crosses by our laboratory, based on a difference in expression or a nonsynonymous coding polymorphism (8). Resequencing verified that the damaging polymorphism did not segregate between MRL and SM (data not shown). *Abca1* was shown to be *cis*-regulated (eQTL on Chr 4@8.8 cM, LOD = 4.1) and was differentially expressed between MRL and SM (−1.6 and −1.7-fold change between MRL vs. SM, $P = 0.003$ and $P = 0.001$ in males and females, respectively) (Fig. 3 and supplementary Table I). However, the expression

TABLE 2. Genome-wide QTL for HDL in the 282 MRL/MpJ × SM/J F2 mice

QTL ^a	Chromosome	Peak (cM) (95% CI) ^b	Peak (Mb) (95% CI) ^b	LOD score (adjusted LOD) ^c	Closest marker	High strain; mode of inheritance	Sex ^d	Overlapping QTL ^e
—	1 ^f	53.6 (25.6–77.6)	124.5 (47.2–172.8)	ns (2.5)	rs13476086	MRL, Dom	MF	New
<i>Hdlq15</i>	1 ^g	81.6 (76.6–83.6)	177.6 (170.5–181.8)	31.3 (ns)	rs13476248	MRL, Add	MF, M, F	<i>Apoa2</i> (25)
—	3 ^f	32.6 (2.0–76.8)	71.3 (3.8–151.2)	ns (2.2)	rs6351657	MRL, Add	MF	New
—	4 ^h	6.6 (2–32.7)	15.2 (3.5–59.6)	2.4 (2.8)	rs13477566	SM, Rec	F	C57BL/6J × NOD/ShiLtJ ⁱ
<i>Hdlq78</i>	4 ^f	20.0 (2.0–31.2)	38.6 (3.5–58.3)	ns (3.8)	rs3702229	SM, Add	MF, M	DBA/2J × CAST/EiJ (46) CAST/EiJ × 129S1/ SvImJ (47)
—	5 ^h	89.1 (38–89.1)	149.8 (71.9–149.8)	2.7 (ns)	rs3710365	MRL, Dom	M	New
—	6 ^h	25.4 (15.5–62.4)	52 (36–127.5)	ns (2.7)	rs3696518	MRL, SM, Dom	F	NZB/BINJ × SM/J (35) B6 × NOD/ShiLtJ ⁱ
<i>Hdlq79</i>	7 ^f	31.1 (14.1–62.1)	56.3 (27.0–124.1)	ns (4.6)	rs3663313	MRL, Add	MF, F	New
<i>Hdlq80</i>	7 ^f	58.2 (na)	118.6 (ns)	ns	rs3711721	—	MF	C57BL/6J × NOD/ShiLtJ ⁱ
—	9 ^h	72.2 (16.8–72.2)	120.9 (31.1–120.9)	ns (2.2)	rs13480455	MRL, Add	M	New
—	10 ^g	30.9 (10.9–40.9)	60.0 (23.4–82.6)	2.5 (ns)	rs13480652	Het, —	MF, M	New
<i>Hdlq81</i>	11 ^g	43.7 (34.7–55.7)	71.7 (56.9–90.6)	2.4 (4.1)	rs3024185	MRL, Dom	MF, F	C57BL/6J × C3H/HeJ (48)
—	13 ^h	33.6 (25.3–49.3)	63.8 (49.6–96.0)	3.8 (ns)	rs13481811	MRL/SM, — (Female)	MF, F	C57BL/6J.C-H25c × BALB/cJ (49)
—	14 ^h	18.9 (10.3–32.9)	31.5 (20.5–62.1)	3.3 (3.4)	rs13482172	SM, Add	F	SM/J × A/J (50)
<i>Hdlq82</i>	18 ^g	42.3 (32.3–54.0)	68.6 (58.3–81.0)	3.5 (4.4)	rs2955992	MRL, Dom	MF, M	NZB/BINJ × NZW/LacJ (51) C57BL/6J × C3H (48) C57BL/6J × DBA/2J (52)
—	19 ^h	50.6 (5–50.6)	55.1 (6.5–55.1)	2.6 (ns)	rs3654713	MRL, Dom	F	

Chr, chromosome; CI, confidence interval; ns, nonsignificant; Het, heterozygotes; M, males; F, females; MF, males + females.

^a HDL QTL were named following the recommendations of MGI (53).

^b 95% CI. Genome-wide significance levels were determined by permuting the observed data 1,000 times. CI was calculated with the Bayesian method. In the combined sex analysis, for the autosomes, the significant and suggestive thresholds were 3.6 and 2.2, respectively. For the X chromosome, the significant and suggestive thresholds were 3.4 and 2.0, respectively. In the sex-specific analysis, for the autosomes, the significant and suggestive thresholds were 3.6 and 2.2, respectively in males and females. For the X chromosome, the significant and suggestive thresholds were 2.7 and 1.4, respectively, in males and 2.8 and 1.5, respectively, in females. When the QTL was identified in both males and females (MF) and in one sex only (sex-specific QTL), we only report the location of the peak and 95% CI in the males + females population.

^c LOD scores were calculated with sex as an additive covariate in the males + females (MF) analysis except for the QTL on chromosome 13, where sex was added as an interactive covariate. HDL was further adjusted for the *Apoa2* locus on chromosome 1 by adding rs13476248 as an additive covariate. The LOD scores in parentheses indicate the LOD score after the *Apoa2* locus adjustment. Bold indicates significant QTL.

^d QTL analysis was run in males (M) and females (F) separately. MF indicates that the QTL was found in the entire F2 population using sex as an additive or interactive covariate. If the peak of the QTL in the combined sex analysis was also observed in the sex-specific analysis, the sex in which the QTL was found is indicated.

^e Overlapping QTL: Peaks within 10 Mb of the MRL×SM peak were selected. The high HDL allele is indicated in bold.

^f HDL QTL after adjustment of HDL with the *Apoa2* locus on chromosome 1 by adding rs13476248 as an additive covariate. Sex was added as an additive covariate in the males + females population.

^g HDL QTL prior to adjustment of HDL with the *Apoa2* locus on chromosome 1. Sex was added as an additive covariate in the males + females population.

^h Sex-specific QTL. QTL identified by either adding sex as an additive and interactive covariate in the males + females population or by QTL analysis in males or females only.

ⁱ Su et al., unpublished data.

^j Interactive QTL.

of *Abca1* was not found to be causal of the chromosome 4 HDL QTL (see supplementary Table II), and the expression of *Abca1* only correlated with HDL^{*Apoa2*} in females ($r = 0.24$, $P = 0.005$), not in the entire F2 population (see supplementary Table I). Therefore, while we found some evidence for *Abca1* as a candidate gene for the chromosome 4 HDL QTL, we suspect that other genes located on chromosome 4 proximal are yet to be identified, as indicated in supplementary Table I.

On chromosome 18, eight crosses have previously identified an HDL QTL on distal chromosome 18 (26). Two well-known lipid genes are present in this region: *Ppargc1b* (peroxisome proliferative activated receptor γ , coactivator 1 β) and *Lipg* (lipase, endothelial). *Ppargc1b*, located at 61.5 Mb, carries an amino acid change (D575N) (Fig. 2 and supplementary Table I). The polymorphism is predicted to be tolerated (SIFT) and is hypothesized to be

responsible for the HDL and TG QTL in the NZB×NZW/LacJ (NZW) cross on a high-fat diet (27). *Ppargc1b* knockout mice show no difference in HDL when fed a chow diet. Because the MRL×SM F2 mice were fed chow (28), we consider *Ppargc1b* to be an unlikely QTL gene for this cross. *Lipg* is located at 75 Mb on chromosome 18, and a change in expression is thought to be responsible for the QTL of three crosses (B6×D2, NZB/BINJ×SM/J [NZB×SM], B6×C3H) (26). Because of the known role of *Lipg* in HDL regulation and its close location to the MRL×SM chromosome 18 QTL, we investigated whether it could be responsible for our QTL. We investigated the microarray results, but did not find a significant difference in expression between MRL and SM or any eQTL for *Lipg* (see supplementary Table I). However, we identified a nonsynonymous coding polymorphism (V118I) through resequencing of the coding regions (Fig. 3). This polymorphism is highly

TABLE 3. Regression ANOVA for HDL in the F2 mice

Sex ^a	Chromosome (cM) ^b	df	% Variance ^c	F	P
M+F	Sex	1	47.3	648.6	$<2.0 \times 10^{-16}$
	Chr1@54cM	2	0.8	5.6	4.2×10^{-3}
	Chr1@81.6cM	2	10.9	74.8	$<2.0 \times 10^{-16}$
	Chr4@20.0cM	2	0.9	6.5	1.7×10^{-4}
	Chr7@35.2cM	2	1.4	9.9	6.9×10^{-6}
	Chr10@31.9cM	2	0.9	6.5	1.7×10^{-3}
	Chr11@42.8cM	2	0.8	5.8	3.2×10^{-3}
	Chr18@40.3cM	2	0.7	5.2	1.0×10^{-3}
	Total	15	63.7		
M	Chr1@73.5cM	2	33.5	49.0	$<2.0 \times 10^{-16}$
	Chr4@14.0cM	2	3.5	5.1	7.2×10^{-3}
	Chr7@23.4cM	2	5.2	7.5	7.8×10^{-4}
	Chr9@68.8cM	2	4.2	6.1	2.8×10^{-3}
	Chr18@32.2cM	2	3.5	5.1	7.0×10^{-3}
	Total	8	49.9		
F	Chr1@85.8cM	2	42.2	75.4	$<2.0 \times 10^{-16}$
	Chr6@29.4cM	2	4.2	7.5	8.1×10^{-4}
	Chr7@39.2cM	2	4.3	7.7	6.9×10^{-4}
	Chr11@43.5cM	2	4.5	8.0	5.4×10^{-4}
	Chr14@25.1cM	2	4.2	7.5	8.6×10^{-4}
	Total	12	59.4		

^a Regression analysis was performed in the entire F2 population ($n = 282$) using sex as an additive covariate or in males and females separately.

^b Sex-specific positions were used in the regression analysis for males and females only as provided on the CGD website.

^c All QTL and interactive QTL were fitted into a model for HDL. Any QTL that did not reach the threshold of 0.001 were removed.

conserved and has not been reported previously (Fig. 3). V118I is also estimated to be damaging (using Polyphen and SIFT). The isoleucine is specific to the SM strain, whereas all the other strains involved in a cross that showed an HDL QTL on chromosome 18 carry a valine (Fig. 3). Therefore, we hypothesize that this polymorphism is responsible for the chromosome 18 HDL QTL from the MRL×SM cross in addition to the HDL QTL from the NZB×SM and LG×SM crosses (26, 29). Further in vitro experiments will be necessary to validate the functionality of the polymorphism.

WGCNA

We performed gene co-expression network analysis on 22,120 transcripts from the liver microarray in the 282 F2 mice, males only and females only (12). Each transcript represented a unique gene and was selected based on high connectivity if a gene was represented by more than one transcript on the microarray. We identified 14, 23, and 20 co-expression modules in the F2, male, and female cohorts respectively (Table 4). The higher numbers of modules in the male- and female-only populations may be explained by the lower numbers of mice compared with the entire F2 population. Each module varied in size from 185 to 5,059 genes in the F2 mice, from 123 to 6,354 in males, and from 122 to 5,112 in females. We identified 8,562, 7,446, and 8,266 genes that did not cluster in any modules in the F2, male, and female cohorts, respectively. We then examined the correlation between the eigengene of the module with HDL and HDL^{Apoa2}. We identified two modules in the entire cohort (brown) that negatively and significantly correlated with HDL^{Apoa2} ($r = -0.18$, $P = 0.002$) (Table 4). We also identified four modules in males (dark-green, light-green, salmon, and yellow) and two modules in females (pink and royal blue) that correlated

with HDL^{Apoa2} ($P < 0.05$) (Table 4). The brown module in the F2 population was composed of 770 genes; 528 of these were common to the male yellow module and 227 were common to the female pink module (see supplementary Tables III, IV). We investigated the functionality of the module correlated with HDL^{Apoa2} using Gene Ontology (Table 5). The F2 brown, male yellow, male salmon, and female pink modules were enriched for genes related to the immune system with $P_{Bonferroni}$ between 5.03×10^{-10} and 2.74×10^{-45} (Table 5). In females, the royal blue module was enriched with genes involved in sterol and lipid biosynthetic process with $P_{Bonferroni}$ between 2.07×10^{-18} and 3.82×10^{-23} . In males, the dark-green module was enriched with genes involved in the FA biosynthetic process ($P_{Bonferroni} = 0.006$) and the light-green module was enriched with genes involved in cell adhesion ($P_{Bonferroni} = 2.7 \times 10^{-8}$).

Genomic dissection of the HDL-related module QTL and identification of candidate genes for the module and the chromosome 11 HDL QTL

We investigated the underlying genetics of the modules correlated with HDL^{Apoa2} in the F2 mice and in males and females only by performing a QTL analysis using the module eigengene as the phenotype (Table 6). We identified a significant QTL on chromosome 11 for which the confidence interval overlaps between the brown module in males and females (Chr 11@28.8 cM, LOD = 9.0), the yellow module in males (Chr 11@44.8 cM, LOD = 5.1), and the pink module in females (Chr 11@29.8cM, LOD = 6.9) (Fig. 4). The QTL plot indicates multiple peaks on chromosome 11, with one common overlapping peak at about 45 cM (Fig. 4). In males only, we also identified two significant QTL on Chr 1@74.6 cM (LOD = 5.3) and Chr 6@41.6 cM (LOD = 5.7) for the

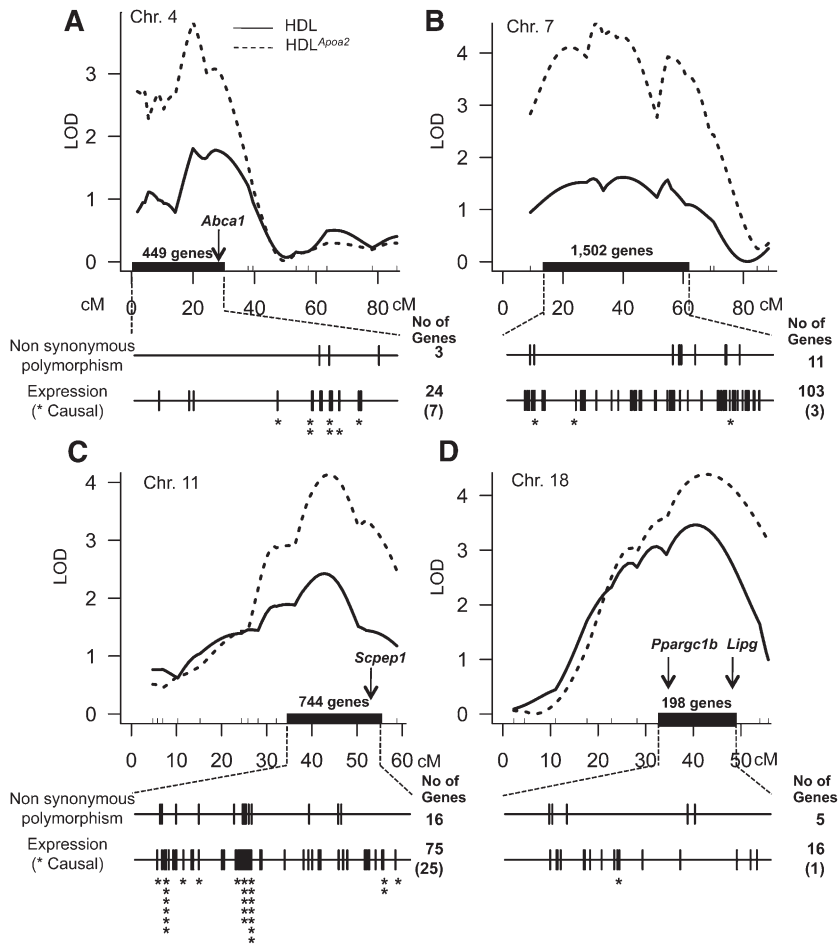


Fig. 2. Genomic dissection of the significant HDL QTL adjusted for *ApoA2* using our bioinformatics tool. Panels show the QTL plots for chromosomes 4 (A), 7 (B), 11 (C), and 18 (D) for HDL (solid line) and HDL^{ApoA2} (dotted line). Each 95% confidence interval is indicated with a thick black line. Using bioinformatics, we reduced the confidence interval to a few genes for each QTL based on the presence of molecular evidence indicated below each QTL plot: either a nonsynonymous coding polymorphism between MRL and SM (upper line) or a differential expression of a gene between the strains (gene differentially expressed between MRL and SM, gene expression *cis*-regulated and correlated with HDL^{ApoA2}) (lower line). Each gene is indicated at its physical location by a vertical line; the total number of genes is indicated as well. Each star indicates a gene for which the expression was found to be causal to the QTL; the total number of “causal” genes is indicated in parentheses. Some of these stars overlap due to the close proximity of the genes and the scale of the figure.

dark-green module, and one significant QTL on Chr 17@16 cM (LOD = 5) for the salmon module (Table 4). No significant QTL was identified for the light-green module in males and the royal-blue module in females. Considering

that 1) the brown module is genetically determined by a major overlapping QTL on chromosome 11, also found in males (yellow module) and females (pink module) (Fig. 4), 2) their module eigengenes are significantly

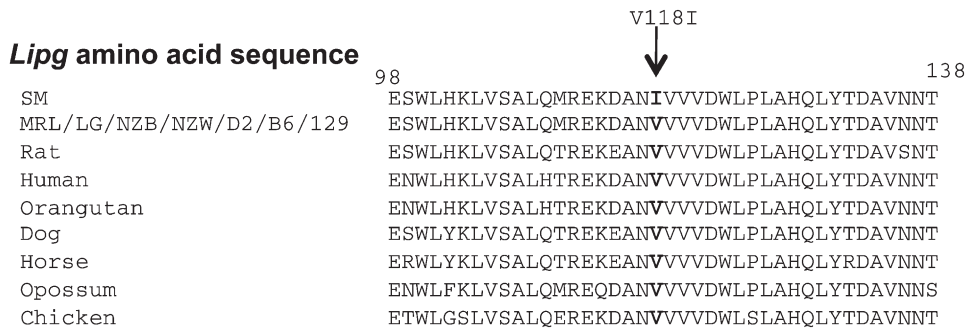


Fig. 3. *Lipg* amino acid sequence alignment. The sequences were obtained from the University of California at Santa Cruz website. The novel polymorphism is indicated in bold.

TABLE 4. WGCNA using 22,120 transcripts in the 282 F2 mice, males and females separately

Module ^a	Males + females				Males				Females			
	No. genes	Correlation ^b R, P		Module ^a	No. genes	Correlation R, P		Module ^a	No. genes	Correlation R, P		
		HDL	HDL ^{Δ^{pmc2}}			HDL	HDL ^{Δ^{pmc2}}			HDL	HDL ^{Δ^{pmc2}}	
Pink	404	0.073 (0.2)	0.019 (0.8)	Turquoise	6,354	0.11 (0.2)	0.049 (0.6)	Yellow	489	0.12 (0.2)	0.081 (0.3)	
Brown	770	-0.62 (0.3)	-0.18 (0.002)	Brown	808	0.056 (0.5)	-0.021 (0.8)	Black	358	0.02 (0.8)	0.12 (0.2)	
Red	461	0.036 (0.6)	-0.066 (0.3)	Green-yellow	315	0.02 (0.8)	-0.053 (0.5)	Grey60	152	0.022 (0.8)	0.093 (0.3)	
Blue	3,849	-0.04 (0.5)	0.025 (0.7)	Black	399	-0.069 (0.4)	-0.13 (0.1)	Magenta	337	0.08 (0.4)	0.046 (0.6)	
Salmon	185	-0.003 (1)	0.017 (0.8)	Midnight blue	270	-0.087 (0.3)	-0.07 (0.4)	Blue	3,351	0.035 (0.7)	0.064 (0.4)	
Magenta	368	0.042 (0.5)	-0.046 (0.4)	Cyan	278	-0.13 (0.1)	-0.099 (0.2)	Green	452	0.027 (0.8)	0.079 (0.4)	
Black	407	-0.054 (0.4)	-0.078 (0.2)	Pink	399	-0.14 (0.1)	-0.068 (0.4)	Midnight blue	231	0.075 (0.4)	-0.036 (0.7)	
Green-yellow	231	-0.021 (0.7)	-0.029 (0.6)	Dark-red	123	-0.01 (0.9)	0.076 (0.4)	Green-yellow	305	0.053 (0.5)	-0.11 (0.2)	
Green	591	0.053 (0.4)	-0.006 (0.9)	Magenta	365	0.12 (0.1)	0.00 (1)	Pink	340	-0.059 (0.5)	-0.26 (0.003)	
Turquoise	5,059	0.045 (0.4)	0.011 (0.8)	Dark-green	109	0.031 (0.7)	0.28 (5.0E-4)	Brown	533	-0.015 (0.9)	-0.003 (0.7)	
Yellow	696	0.037 (0.5)	-0.13 (0.8)	Tan	305	0.065 (0.4)	0.092 (0.3)	Cyan	262	-0.031 (0.7)	-0.011 (0.9)	
Purple	345	0.014 (0.8)	-0.01 (0.9)	Royal blue	138	0.023 (0.8)	0.15 (0.06)	Light-yellow	152	0.058 (0.5)	-0.043 (0.6)	
Tan	192	0.001 (1)	-0.06 (0.3)	Red	418	0.007 (0.9)	0.11 (0.2)	Light-green	152	-0.007 (0.9)	-0.033 (0.7)	
				Blue	1,760	-0.078 (0.3)	0.028 (0.7)	Tan	270	0.11 (0.2)	0.022 (0.8)	
				Green	443	-0.12 (0.1)	-0.063 (0.4)	Turquoise	5,112	-0.036 (0.7)	-0.059 (0.5)	
				Dark-turquoise	100	0.054 (0.5)	0.037 (0.7)	Red	446	0.018 (0.8)	0.0054 (1)	
				Grey60	177	-0.089 (0.3)	-0.11 (0.2)	Salmon	264	0.043 (0.6)	0.062 (0.5)	
				Light-cyan	239	-0.062 (0.5)	0.031 (0.7)	Royal blue	122	0.099 (0.3)	0.17 (0.05)	
				Light-yellow	147	-0.18 (0.04)	-0.11 (0.2)	Light-cyan	202	-0.075 (0.4)	-0.025 (0.8)	
				Purple	358	0.09 (0.3)	0.029 (0.7)	Purple	324	-0.022 (0.8)	0.054 (0.5)	
				Light-green	158	-0.096 (0.2)	-0.17 (0.04)					
				Salmon	299	-0.062 (0.5)	-0.23 (0.006)					
				Yellow	712	-0.1 (0.2)	-0.19 (0.02)					

^a Modules identified using the WGCNA using the 22,120 transcripts. If more than one transcript represented a gene, the transcript with the highest connectivity in the 282 F2 mice dataset was chosen. Each module was assigned a color.

^b Correlation between the eigengenes of each module and HDL and HDL^{Δ^{pmc2}} (12). Significant correlations are indicated in bold. The genes that do not cluster with any modules are assigned to the gray module, which is not represented here.

TABLE 5. Gene Ontology results of the modules correlated with HDL^{Apoa2}

Modules	GO reference ^a	GO functions annotation	Term ontology ^b	Number of molecules	Enrichment	
2.30E-22 Bonferroni <i>P</i>						
Males and Females						
Brown	GO:0002376	Immune system process	BP	129	3.04E-49	2.74E-45
	GO:0006955	Immune response	BP	80	1.06E-34	9.51E-31
	GO:0002682	Regulation of immune system process	BP	63	2.97E-29	2.68E-25
	GO:0006952	Defense response	BP	73	1.61E-27	1.45E-23
	GO:0001775	Cell activation	BP	58	2.19E-23	1.97E-19
Males						
Dark-green	GO:0006633	FA biosynthetic process	BP	7	6.83E-07	0.006
	GO:0006631	FA metabolic process	BP	9	7.90E-07	0.007
Light-green	GO:0005576	Extracellular region	CC	1527	1.81E-26	1.63E-22
	GO:0031012	Extracellular matrix	CC	282	2.91E-26	2.62E-22
Salmon	GO:0005578	Proteinaceous extracellular matrix	CC	262	5.90E-26	5.32E-22
	GO:0044421	Extracellular region part	CC	625	7.99E-25	7.21E-21
	GO:0007155	Cell adhesion	BP	551	2.99E-12	2.70E-08
	GO:0002376	Immune system process	BP	43	5.58E-14	5.03E-10
	GO:0019882	Antigen processing and presentation	BP	13	6.58E-14	5.93E-10
Yellow	GO:0048002	Antigen processing and presentation of peptide antigen	BP	11	1.53E-13	1.38E-09
	GO:0050776	Regulation of immune response	BP	21	6.92E-13	6.24E-09
	GO:0002682	Regulation of immune system process	BP	26	7.51E-13	6.77E-09
	GO:0002376	Immune system process	BP	745	1.00E-34	9.01E-31
	GO:0006955	Immune response	BP	403	2.15E-23	1.94E-19
Females	GO:0009897	External side of plasma membrane	CC	148	1.67E-17	1.51E-13
	GO:0001775	Cell activation	BP	318	1.99E-17	1.79E-13
	GO:0009986	Cell surface	CC	226	2.21E-16	2.00E-12
Pink	GO:0002376	Immune system process	BP	68	2.50E-30	2.25E-26
	GO:0048002	Antigen processing and presentation of peptide antigen	BP	18	1.33E-25	1.20E-21
	GO:0006955	Immune response	BP	46	1.42E-24	1.28E-20
	GO:0019882	Antigen processing and presentation	BP	20	3.81E-24	3.44E-20
	GO:0019884	Antigen processing and presentation of exogenous antigen	BP	14	1.29E-18	1.16E-14
Royal blue	GO:0016126	Sterol biosynthetic process	BP	16	4.24E-27	3.82E-23
	GO:0008610	Lipid biosynthetic process	BP	27	1.50E-24	1.35E-20
	GO:0016125	Sterol metabolic process	BP	18	9.72E-24	8.76E-20
	GO:0006694	Steroid biosynthetic process	BP	17	1.53E-22	1.38E-18
	GO:0006695	Cholesterol biosynthetic process	BP	13	2.30E-22	2.07E-18

^a Bioconductor was used to identify common functions among the genes from the brown module in the F2 mice. Only the top five GO functional annotations are indicated here.

^b BP, biological process; CC, Cellular Component.

correlated with HDL^{Apoa2} (Table 4), and 3) this major module QTL overlaps with a significant HDL^{Apoa2} QTL (Table 5), we used conditional genome scans to investigate the genes located under the chromosome 11 QTL as potential major players in HDL metabolism. For the chromosome 11 HDL^{Apoa2} QTL, we had originally identified 25 candidate genes based on conditional analysis (Fig. 2, **Table 7** and supplementary Table I). Among the 770 genes from the brown module, 34 were located in the 95% confidence interval of the chromosome 11 brown mQTL (see supplementary Table V). By conditioning the expression of the 34 transcripts on the eigengene, we identified three genes for which the expression was “causative” of the brown mQTL on chromosome 11 (Table 7): *Igrrm* (immunity-related GTPase fam-

ily), *Fbxo39* (F-box protein 39), and *Slfn5* (schlafen 5). Although none of these genes were found to be causal for the chromosome 11 HDL^{Apoa2} QTL, our criteria are stringent, and thus we cannot exclude the possibility that one of the candidate genes is responsible for both the HDL^{Apoa2} QTL and the brown mQTL. Additionally, we searched for candidate genes for the mQTL found in males (yellow) and females (pink) separately based on conditional genome scans (see supplementary Table VI). We identified five genes that were also found to be causal to the chromosome 11 HDL^{Apoa2} QTL in males or females: *Mpdu1* (mannose-P-dolichol utilization defect 1), *Rnasek* (RNase, RNase K), *Fbxo39* (F-box protein 39) in males, and *Ulk2* (Unc-51 like kinase 2 (*C. elegans*)) and *Gltpd2* (glycolipid transfer protein

TABLE 6. Module QTL (mQTL) correlated with HDL^{Apoa2}

Sex	Modules	mQTL ^a peak (95% CI) (cM)	LOD
Males + females	Brown	Chr 11@28.8 (26.8–57.8)	9.0
Males	Dark-green	Chr 1@74.6 (68.6–88.6)	5.3
		Chr 6@41.6 (30.6–52.6)	5.7
	Light-green	None	ns
	Salmon	Chr 17@15.0 (7.9–23.9)	4.3
	Yellow	Chr 11@44.8 (16.8–57.8)	5.1
Females	Pink	Chr 11@29.8 cM (26.8–57.8)	6.9
	Royal blue	None	ns

^a For the modules significantly correlated with HDL^{Apoa2}, QTL analysis was run using the module eigengene as the phenotype. Significant mQTL (LOD > 3.7 for males + females and males only; LOD > 3.6 for females only) are reported here with the 95% confidence interval and the LOD score.

domain containing 2) in females (see supplementary Table VI). Finally, we identified two candidate genes for the chromosome 1 dark-green mQTL (*Fh1*, fumarate hydratase 1 and *Degs1*, degenerative spermatocyte homolog 1 (*Drosophila*)) and two genes for the chromosome 17 salmon mQTL (*Slc37a1*, solute carrier family 37 (glycerol-3-phosphate transporter), member and *H2-T23*, histocompatibility 2, T region locus 23) in males (see supplementary Table VI). None of these genes are known to be involved in HDL metabolism.

DISCUSSION

In this study, we performed QTL mapping for HDL using an intercross between two strains with highly different HDL levels, MRL and SM. We identified eight new QTL on chromosomes 1 (middle), 3, 4, 7 (proximal), 10, 11, 13, and 18, and confirmed two QTL on chromosomes 1 (distal) and 7 (distal). We then applied our bioinformatic tool to identify candidate genes located under the strongest QTL on chromosomes 4, 7, 11, and 18. We specifically searched for genes that either carry a nonsynonymous coding polymorphism or differ in expression between the

parental strains, and that are *cis*-regulated, correlate with HDL, and are likely to be causal to the QTL.

By choosing two strains with highly different levels of HDL-cholesterol, we ensured that we would identify the most important regulator of HDL-cholesterol between these two strains, but we could not predict the number of QTL we would identify. We expected a QTL on distal chromosome 1 for HDL-cholesterol, inasmuch as MRL and SM differ in their haplotype at the locus (25). However, the LOD score was unusually strong. The adjustment of HDL with the *Apoa2* locus allowed us to identify additional QTL that may have been masked by the chromosome 1 QTL. This approach confirmed the suggestive QTL found in the analysis before conditioning (chromosomes 11 and 18) and identified additional QTL on chromosomes 3 and 4. While the QTL on chromosomes 11 and 18 were found both before and after adjustment for *Apoa2*, however, the chromosome 10 QTL and the female-specific QTL on chromosome 13 were not replicated after the adjustment. We hypothesize that the lower nonsignificant LOD score after adjustment for *Apoa2* may reflect an interaction between the *Apoa2* locus and the chromosome 10 QTL and between the *Apoa2* locus and the chromosome 13 QTL. This interaction would not have been statistically detectable prior to adjustment because of the strong LOD score at the *Apoa2* locus. In addition, a strong QTL may indicate the presence of more than one QTL gene. Recently, Lawson et al. (30) reported the results of an F16 generation between LG/J (LG) and SM/J. LG is closely related to MRL. In this report, two different QTL were identified on chromosome 1 at 173.1 and 179.1 Mb for total cholesterol. While the first QTL at 173.1 Mb is likely to be due to the *Apoa2* gene, the authors identified several candidate genes for the second QTL. The resolution of our cross (F2) does not allow us to separate these two possible QTL on chromosome 1, but the large LOD score may be an indication of more than one QTL gene at this locus. In fact, we identified *Fh1* at 177.5 Mb as a candidate gene for the dark-green HDL-related module in males. This gene had previously been identified as a candidate gene in an NZB/BINJ × SM cross based on differential gene expression and protein abundance between the parental strains (31) and could be an additional candidate gene for the chromosome 1 HDL QTL.

As previously shown in our study on triglycerides using the same mouse F2 cross (13), the identification of a causal QTL gene is based on a bioinformatic approach that considers the molecular basis of a QTL to be a differential

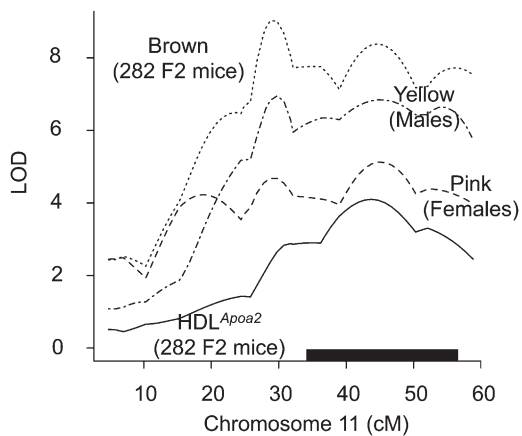


Fig. 4. Chromosome 11 QTL plot for HDL^{Apoa2} and mQTL plots for the brown (males and females), yellow (males), and pink (females) modules. chromosome 11 QTL for HDL^{Apoa2} level and the brown mQTL in 282 F2 mice are indicated in solid and dotted lines, respectively. chromosome 11 mQTL for the yellow module in males and the pink module in females are indicated by the dashed-dotted and dashed lines, respectively. QTL analysis is described in Fig.1. The confidence interval of the HDL^{Apoa2} is indicated by a thick black line.

TABLE 7. Conditional linkage analysis for the HDL QTL and module QTL on chromosome 11

Gene ^a	Pos. (Mb)	HDL ^{Apoa2} QTL ^{a,b}		eQTL ^{c,d}			Brown mQTL ^{a,b}		eQTL ^{c,d}		
		LOD	LOD ^{a,d,j, b}	Loc.(cM)	LOD	LOD ^{a,d,j, c}	LOD	LOD adj ^b	Loc.(cM)	LOD	LOD adj ^c
<i>Irgm</i>	48.7	4.1	na	na	na	na	9.0	1.5	11@44.8	11.4	2.7
<i>Snab47</i>	59.2		1.1	11@37.8	75.7	72.8		na	na	na	na
<i>Flcn</i>	25.6		2.7	11@39	12.4	10.9		na	na	na	na
<i>Atpaf2</i>	60.2		1.8	11@37.8	43.5	41.3		na	na	na	na
<i>Llgl1</i>	60.5		1.6	11@37.8	37.5	35.1		na	na	na	na
<i>Flil</i>	60.5		2.1	11@37.8	53.9	51.9		na	na	na	na
<i>Smcr7</i>	60.5		1.2	11@37.8	41	38.3		na	na	na	na
<i>Smcr8</i>	60.6		1.6	11@37.8	22.3	19.9		na	na	na	na
<i>Shmt1</i>	60.6		2	11@36.8	34.3	32.3		na	na	na	na
Ulk2	61.6		1.6	11@37.8	74.3	71.8		na	na	na	na
<i>2310004124Rik</i>	66.9		1.9	11@41.8	26.5	24.3		na	na	na	na
<i>Rpl26</i>	68.7		2.1	11@42.8	62.2	60.2		na	na	na	na
<i>Chd3</i>	69.2		0.9	11@42.8	56.5	53.3		na	na	na	na
<i>Sat2</i>	69.4		0.8	11@43.8	42.1	38.7		na	na	na	na
Mpdu1	69.5		2	11@41.8	26.3	24.1		na	na	na	na
<i>Asgr1</i>	69.9		2	11@44.8	20.1	18		na	na	na	na
<i>Asgr2</i>	69.9		0.5	11@43.8	60.4	56.6		na	na	na	na
Rnasek	70.1		1.8	11@42.8	44.8	42.5		na	na	na	na
<i>Med11</i>	70.3		1.9	11@43.8	19.6	17.4		na	na	na	na
Glt3pd2	70.3		0.4	11@43.8	62.7	58.5		na	na	na	na
<i>Clqbp</i>	70.8		1.6	11@45.8	21.2	18.8		na	na	na	na
<i>Dhx33</i>	70.8		2.2	11@45.8	15.2	13.3		na	na	na	na
<i>Mis12</i>	70.8		0.9	11@43.8	39.1	35.8		na	na	na	na
<i>6330403K07Rik</i>	70.8		1.5	11@46.8	24	21.4		na	na	na	na
Fbxo39	72.1		na	na	na	na		1.3	11@45.8	13	4.8
<i>Slfn5</i>	82.7		na	na	na	na		1.7	11@45.8	11.2	3.4
<i>Scpep1</i>	88.8		1.8	11@54.8	54.5	52.3		na	na	na	na
<i>Gm15698</i>	88.8		1.9	11@47.8	25.3	23.2		na	na	na	na
<i>Tom11l</i>	90.5		1.9	11@56.8	30.2	28.2		na	na	na	na

^a Conditional genome scans were performed in the F2 population for HDL^{Apoa2} on the chromosome 11 HDL QTL and the brown module eigengene in the F2 population. To be considered causal, the LOD score of the candidate gene had to be reduced below the suggestive level (LOD < 2.2), and the expression QTL LOD score adjusted for the trait must not have been reduced below the suggestive level. Only the genes showing evidence of causality for HDL^{Apoa2} QTL are reported here, in addition to genes found to be causal for the brown modules. Bold indicates that the gene was also found to be causal in males or females only (see supplementary Table VI).

^b Conditional genome scan on HDL^{Apoa2} in males and females using the expression of the gene as a covariate. na indicates that the gene was not causal of HDL^{Apoa2} or not present in brown module.

^c Conditional genome scan on the gene expression (eQTL) using the phenotypic trait (HDL^{Apoa2} or brown eigengene) as a covariate.

^d *Apoa2* was used as a covariate in the expression QTL analysis here to allow for comparison. Therefore, the position of the *cis* eQTL and LOD score varies slightly compared with the results in supplementary Table 1 but does not affect the outcome: genes stay *cis*-expressed after adjustment for *Apoa2*.

expression of a gene or a nonsynonymous coding polymorphism segregating between the parental strains (25, 32). With this approach, we confirmed known candidate genes. For instance, the HDL QTL on chromosome 18 has been identified in multiple mouse crosses (26); in addition, it is located in orthologous regions in baboons and humans (33, 34). A difference in expression in *Lipg* explained the chromosome 18 HDL QTL in at least three mouse crosses (B6×D2, NZB×SM, B6×C3H) (26). However, we identified a novel nonsynonymous coding polymorphism that is probably responsible for the chromosome 18 QTL in the MRL×SM cross as well as the differences between the SM×NZB (35) and LG×SM crosses (30). In addition, although our approach is a powerful way to identify potential QTL candidate genes, our study reflects the complexity of the identification of QTL genes. The genomic dissection of QTL is usually based on the examination of SNP and gene expression databases (36) and relies on the accuracy of the comprehensive public databases. In our study, this type of straightforward examination would have missed the novel polymorphism. Therefore, while our approach is powerful, its success requires careful interpretation of the results of the bioinformatics tools.

By combining traditional genetics approaches and system genetics, we were able to add evidence to candidate genes for the chromosome 11 HDL QTL based on expression differences between the parental strains and causality of not only the HDL QTL but also the HDL-related module QTL. Causal analysis leverages the natural variation that occurs within the segregating populations and the unidirectional relationship between genotype and phenotype. Analysis of this type is widely used to sort out the relationships between complex traits, using QTL as a causal anchor (37). Conditional genome scans are a convenient test for causality within the QTL mapping framework (22). We adopted the genome-wide significance threshold for the causality test, which is stringent. A large drop in LOD score upon conditioning should be viewed as suggestive of a causal relationship.


In our study, we identified a module correlated with HDL and enriched for genes involved in inflammatory response. Proteomics studies have previously identified proteins involved in inflammation, such as complement activation proteins, on HDL particles (38). Among their functions, HDL particles have the capacity to inhibit the adhesion of monocytes to the endothelium and express anti-inflammatory properties (as reviewed in Ref. 39).

These anti-inflammatory properties are known to be proportionate to HDL concentration and affect the TLR4-mediated inflammatory response of macrophages (40). At the genetic level, associations between genetic polymorphisms in genes involved in an inflammatory pathway (such as TNF α) and HDL concentration have been observed previously (41). Here, we found that the eigengene of the brown module was negatively correlated with the expression of inflammatory genes, which corroborates a previous finding: Park et al. (42) showed that HDL downregulates the expression of VCAM-1 in endothelial cells triggered by TNF α . These results show how HDL particles are capable of modulating inflammation response genes. How inflammatory genes could affect HDL-cholesterol level is yet to be determined. However, no direction of causality between the module eigengene and HDL-cholesterol level was identified in our study. Therefore, we hypothesize that one of the candidate genes on chromosome 11 affects HDL-cholesterol level, which in turn affects inflammatory gene expression, leading to the identification of a module enriched for inflammatory response genes, which also correlated with HDL-cholesterol level.

With the exception of *ApoA1* and *Lipg*, none of the candidate genes are known to play a role in HDL metabolism or were identified in recent human genome-wide association analysis for HDL-cholesterol (6). This latter finding may indicate a difference in the genetics of HDL metabolism between mice and humans. However, our group has previously shown that genes regulating HDL-cholesterol are often concordant between mice and humans (7, 8). Mouse intercrosses allow for the identification of QTL due to a specific strain's polymorphisms that have an effect strong enough to be detectable in the F2 population studied. In addition, system genetics approaches allow for the identification of genes with small effects on the phenotype but that may produce larger effects when taken together as a module. Combining both approaches, our study allowed for the identification of genes that may have been undetectable by human genome-wide association analysis due to their small effect or lack of functional polymorphisms in human populations. These genes could in fact explain part of the unexplained inter-individual variation often observed in human genome-wide association analysis. Among the candidate genes on chromosome 11, *Atpaf2* (ATP synthase mitochondrial F1 complex assembly factor 2) was identified in a human GWAS for gallstone disease, a phenotype related to cholesterol metabolism, with a polymorphism at a statistically marginal level ($P < 10^{-3}$, ranked = 203) within 10 Kb of the gene (43). The gene encodes for a factor involved in the assembly of F(1) component of the mitochondrial ATP synthase. The β chain of ATP synthase has been shown to bind to apoA-1 and to induce the internalization of HDL particles (44), which makes *Atpaf2* a major candidate gene for the chromosome 11 HDL QTL. The direct or indirect link between *Atpaf2* and inflammation is yet to be determined.

Finally, HDL particles are mainly synthesized in the liver and the small intestine (45). Because our overall intercross study included not only HDL-cholesterol but also other complex traits (13, 14), we elected to collect the livers in

the parental and F2 mice for microarray expression studies as the major tissue for metabolic processes. However, the examination of expression-level differences in the small intestine could have led to additional candidate genes.

To conclude, we identified known and novel QTL for HDL-cholesterol in mice. Although numerous genes had previously been identified for HDL-cholesterol through human and animal studies, we showed that new genes regulating HDL-cholesterol are yet to be discovered. These novel genes are not the usual suspects, inasmuch as they may be related to new functions of HDL-cholesterol particles, adding complexity to gene identification. Still, expression differences, genomic databases, bioinformatics tools, and system genetics approaches allow us to narrow the list of candidate genes and thus facilitate identification of causal genes. Identifying novel genes for HDL-cholesterol will provide new targets for drug development and will help improve treatments for CAD. 

Note added in proof

The GO analysis for the Royal blue module in Females was missing from Table 5 in the accepted article online. This information has since been added and appears in the final versions of the article in print and online.

The authors thank Harry Whitmore for his help with mouse husbandry, Joanne Curren for editing the manuscript, and Jesse Hammer for graphical assistance.

REFERENCES

1. Hopkins, P. N., and R. R. Williams. 1981. A survey of 246 suggested coronary risk factors. *Atherosclerosis*. **40**: 1–52.
2. Castelli, W. P., J. T. Doyle, T. Gordon, C. G. Hames, M. C. Hjortland, S. B. Hulley, A. Kagan, and W. J. Zukel. 1977. HDL cholesterol and other lipids in coronary heart disease. The cooperative lipoprotein phenotyping study. *Circulation*. **55**: 767–772.
3. Barter, P. J., M. Caulfield, M. Eriksson, S. M. Grundy, J. J. Kastelein, M. Komajda, J. Lopez-Sendon, L. Mosca, J. C. Tardif, D. D. Waters, et al. 2007. Effects of torcetrapib in patients at high risk for coronary events. *N. Engl. J. Med.* **357**: 2109–2122.
4. Melnikova, I. 2005. Raising HDL cholesterol. *Nat. Rev. Drug Discov.* **4**: 185–186.
5. Williams, P. T. 1997. Interactive effects of exercise, alcohol, and vegetarian diet on coronary artery disease risk factors in 9242 runners: the National Runners' Health Study. *Am. J. Clin. Nutr.* **66**: 1197–1206.
6. Teslovich, T. M., K. Musunuru, A. V. Smith, A. C. Edmondson, I. M. Stylianou, M. Koseki, J. P. Pirruccello, S. Ripatti, D. I. Chasman, C. J. Willer, et al. 2010. Biological, clinical and population relevance of 95 loci for blood lipids. *Nature*. **466**: 707–713.
7. Wang, X., and B. Paigen. 2005. Genetics of variation in HDL cholesterol in humans and mice. *Circ. Res.* **96**: 27–42.
8. Leduc, M. S., M. Lyons, K. Darvishi, K. Walsh, S. Sheehan, S. Amend, A. Cox, M. Orho-Melander, S. Kathiresan, B. Paigen, et al. 2011. The mouse QTL map helps interpret human genome-wide association studies for HDL cholesterol. *J. Lipid Res.* **52**: 1139–1149.
9. Burgess-Herbert, S. L., A. Cox, S. W. Tsaih, and B. Paigen. 2008. Practical applications of the bioinformatics toolbox for narrowing quantitative trait loci. *Genetics*. **180**: 2227–2235.
10. DiPetrillo, K., X. Wang, I. M. Stylianou, and B. Paigen. 2005. Bioinformatics toolbox for narrowing rodent quantitative trait loci. *Trends Genet.* **21**: 683–692.
11. Langfelder, P., L. W. Castellani, Z. Zhou, E. Paul, R. Davis, E. E. Schadt, A. J. Lusis, S. Horvath, and M. Mehrabian. 2012. A systems genetic analysis of high density lipoprotein metabolism and network preservation across mouse models. *Biochim. Biophys. Acta*. **1821**: 435–447.

12. Langfelder, P., and S. Horvath. 2008. WGCNA: an R package for weighted correlation network analysis. *BMC Bioinformatics*. **9**: 559.
13. Leduc, M. S., R. S. Hageman, R. A. Verdugo, S. W. Tsaih, K. Walsh, G. A. Churchill, and B. Paigen. 2011. Integration of QTL and bioinformatic tools to identify candidate genes for triglycerides in mice. *J. Lipid Res.* **52**: 1672–1682.
14. Leduc, M. S., R. S. Hageman, Q. Meng, R. A. Verdugo, S. W. Tsaih, G. A. Churchill, B. Paigen, and R. Yuan. 2010. Identification of genetic determinants of IGF-1 levels and longevity among mouse inbred strains. *Aging Cell*. **9**: 823–836.
15. Cox, A., C. L. Ackert-Bicknell, B. L. Dumont, Y. Ding, J. T. Bell, G. A. Brockmann, J. E. Wergedal, C. Bult, B. Paigen, J. Flint, et al. 2009. A new standard genetic map for the laboratory mouse. *Genetics*. **182**: 1335–1344.
16. Bolstad, B. M., R. A. Irizarry, M. Astrand, and T. P. Speed. 2003. A comparison of normalization methods for high density oligonucleotide array data based on variance and bias. *Bioinformatics*. **19**: 185–193.
17. Dai, M., P. Wang, A. D. Boyd, G. Kostov, B. Athey, E. G. Jones, W. E. Bunney, R. M. Myers, T. P. Speed, H. Akil, et al. 2005. Evolving gene/transcript definitions significantly alter the interpretation of GeneChip data. *Nucleic Acids Res.* **33**: e175.
18. Broman, K. W., H. Wu, S. Sen, and G. A. Churchill. 2003. R/qtl: QTL mapping in experimental crosses. *Bioinformatics*. **19**: 889–890.
19. Broman, K. W., S. Sen, S. E. Owens, A. Manichaikul, E. M. Southard-Smith, and G. A. Churchill. 2006. The X chromosome in quantitative trait locus mapping. *Genetics*. **174**: 2151–2158.
20. Ng, P. C., and S. Henikoff. 2001. Predicting deleterious amino acid substitutions. *Genome Res.* **11**: 863–874.
21. Li, R., S. W. Tsaih, K. Shockley, I. M. Stylianou, J. Wergedal, B. Paigen, and G. A. Churchill. 2006. Structural model analysis of multiple quantitative traits. *PLoS Genet.* **2**: e114.
22. Neto, E., M. Keller, A. Attie, and B. Yandell. 2010. Causal graphical models in systems genetics: a unified framework for joint inference of causal network and genetic architecture for correlated phenotypes. *Ann. Appl. Stat.* **4**: 320–339.
23. Langfelder, P., and S. Horvath. 2007. Eigengene networks for studying the relationships between co-expression modules. *BMC Syst. Biol.* **1**: 54.
24. Lehmann, E. 1975. Nonparametrics: Statistical Methods Based on Ranks. Holden-Day, San Francisco.
25. Wang, X., R. Korstanje, D. Higgins, and B. Paigen. 2004. Haplotype analysis in multiple crosses to identify a QTL gene. *Genome Res.* **14**: 1767–1772.
26. Su, Z., N. Ishimori, Y. Chen, E. H. Leiter, G. A. Churchill, B. Paigen, and I. M. Stylianou. 2009. Four additional mouse crosses improve the lipid QTL landscape and identify Lipg as a QTL gene. *J. Lipid Res.* **50**: 2083–2094.
27. Su, Z., S. W. Tsaih, J. Szatkiewicz, Y. Shen, and B. Paigen. 2008. Candidate genes for plasma triglyceride, FFA, and glucose revealed from an intercross between inbred mouse strains NZB/B1NJ and NZW/LacJ. *J. Lipid Res.* **49**: 1500–1510.
28. Lelliott, C. J., G. Medina-Gomez, N. Petrovic, A. Kis, H. M. Feldmann, M. Bjursell, N. Parker, K. Curtis, M. Campbell, P. Hu, et al. 2006. Ablation of PGC-1beta results in defective mitochondrial activity, thermogenesis, hepatic function, and cardiac performance. *PLoS Biol.* **4**: e369.
29. Lawson, H. A., A. Lee, G. L. Fawcett, B. Wang, L. S. Pletscher, T. J. Maxwell, T. H. Ehrich, J. P. Kenney-Hunt, J. B. Wolf, C. F. Semenkovich, et al. 2011. The importance of context to the genetic architecture of diabetes-related traits is revealed in a genome-wide scan of a LG/J x SM/J murine model. *Mamm. Genome*. **22**: 197–208.
30. Lawson, H. A., K. M. Zelle, G. L. Fawcett, B. Wang, L. S. Pletscher, T. J. Maxwell, T. H. Ehrich, J. P. Kenney-Hunt, J. B. Wolf, C. F. Semenkovich, et al. 2010. Genetic, epigenetic, and gene-by-diet interaction effects underlie variation in serum lipids in a LG/JxSM/J murine model. *J. Lipid Res.* **51**: 2976–2984.
31. Stylianou, I. M., J. P. Affourtit, K. R. Shockley, R. Y. Wilpan, F. A. Abdi, S. Bhardwaj, J. Rollins, G. A. Churchill, and B. Paigen. 2008. Applying gene expression, proteomics and single-nucleotide polymorphism analysis for complex trait gene identification. *Genetics*. **178**: 1795–1805.
32. Suto, J. 2005. Apolipoprotein gene polymorphisms as cause of cholesterol QTLs in mice. *J. Vet. Med. Sci.* **67**: 583–589.
33. Rainwater, D. L., L. A. Cox, J. Rogers, J. L. VandeBerg, and M. C. Mahaney. 2009. Localization of multiple pleiotropic genes for lipoprotein metabolism in baboons. *J. Lipid Res.* **50**: 1420–1428.
34. Kullo, I. J., S. T. Turner, E. Boerwinkle, S. L. Kardina, and M. de Andrade. 2005. A novel quantitative trait locus on chromosome 1 with pleiotropic effects on HDL-cholesterol and LDL particle size in hypertensive sibships. *Am. J. Hypertens.* **18**: 1084–1090.
35. Korstanje, R., R. Li, T. Howard, P. Kelmenson, J. Marshall, B. Paigen, and G. Churchill. 2004. Influence of sex and diet on quantitative trait loci for HDL cholesterol levels in an SM/J by NZB/B1NJ intercross population. *J. Lipid Res.* **45**: 881–888.
36. Shockley, K. R., D. Witmer, S. L. Burgess-Herbert, B. Paigen, and G. A. Churchill. 2009. Effects of atherogenic diet on hepatic gene expression across mouse strains. *Physiol. Genomics*. **39**: 172–182.
37. Rockman, M. V. 2008. Reverse engineering the genotype-phenotype map with natural genetic variation. *Nature*. **456**: 738–744.
38. Vaisar, T., S. Pennathur, P. S. Green, S. A. Gharib, A. N. Hoofnagle, M. C. Cheung, J. Byun, S. Vuletic, S. Kassim, P. Singh, et al. 2007. Shotgun proteomics implicates protease inhibition and complement activation in the antiinflammatory properties of HDL. *J. Clin. Invest.* **117**: 746–756.
39. Barter, P. J., S. Nicholls, K. A. Rye, G. M. Anantharamaiah, M. Navab, and A. M. Fogelman. 2004. Antiinflammatory properties of HDL. *Circ. Res.* **95**: 764–772.
40. Yvan-Charvet, L., J. Kling, T. Pagler, H. Li, B. Hubbard, T. Fisher, C. P. Sparrow, A. K. Taggart, and A. R. Tall. 2010. Cholesterol efflux potential and antiinflammatory properties of high-density lipoprotein after treatment with niacin or anacetrapib. *Arterioscler. Thromb. Vasc. Biol.* **30**: 1430–1438.
41. Arora, P., B. Garcia-Bailo, Z. Dastani, D. Brenner, A. Villegas, S. Malik, T. D. Spector, B. Richards, A. El-Sohehy, M. Karmali, et al. 2011. Genetic polymorphisms of innate immunity-related inflammatory pathways and their association with factors related to type 2 diabetes. *BMC Med. Genet.* **12**: 95.
42. Park, S. H., J. H. Park, J. S. Kang, and Y. H. Kang. 2003. Involvement of transcription factors in plasma HDL protection against TNF-alpha-induced vascular cell adhesion molecule-1 expression. *Int. J. Biochem. Cell Biol.* **35**: 168–182.
43. Buch, S., C. Schafmayer, H. Volzke, C. Becker, A. Franke, H. von Eller-Eberstein, C. Kluck, I. Bassmann, M. Brosch, F. Lammert, et al. 2007. A genome-wide association scan identifies the hepatic cholesterol transporter ABCG8 as a susceptibility factor for human gallstone disease. *Nat. Genet.* **39**: 995–999.
44. Martinez, L. O., S. Jacquet, J. P. Esteve, C. Rolland, E. Cabezon, E. Champagne, T. Pineau, V. Georgeaud, J. E. Walker, F. Terce, et al. 2003. Ectopic beta-chain of ATP synthase is an apolipoprotein A-I receptor in hepatic HDL endocytosis. *Nature*. **421**: 75–79.
45. Brunham, L. R., J. K. Kruit, J. Iqbal, C. Fievet, J. M. Timmins, T. D. Pape, B. A. Coburn, N. Bissada, B. Staels, A. K. Groen, et al. 2006. Intestinal ABCA1 directly contributes to HDL biogenesis in vivo. *J. Clin. Invest.* **116**: 1052–1062.
46. Lyons, M. A., H. Wittenburg, R. Li, K. A. Walsh, G. A. Churchill, M. C. Carey, and B. Paigen. 2003. Quantitative trait loci that determine lipoprotein cholesterol levels in DBA/2J and CAST/Ei inbred mice. *J. Lipid Res.* **44**: 953–967.
47. Lyons, M. A., H. Wittenburg, R. Li, K. A. Walsh, R. Korstanje, G. A. Churchill, M. C. Carey, and B. Paigen. 2004. Quantitative trait loci that determine lipoprotein cholesterol levels in an intercross of 129S1/SvImJ and CAST/Ei inbred mice. *Physiol. Genomics*. **17**: 60–68.
48. Su, Z., X. Wang, S. W. Tsaih, A. Zhang, A. Cox, S. Sheehan, and B. Paigen. 2009. Genetic basis of HDL variation in 129/SvImJ and C57BL/6J mice: importance of testing candidate genes in targeted mutant mice. *J. Lipid Res.* **50**: 116–125.
49. Welch, C. L., S. Bretschger, P. Z. Wen, M. Mehrabian, N. Latib, J. Fruchart-Najib, J. C. Fruchart, C. Myrick, and A. J. Lusis. 2004. Novel QTLs for HDL levels identified in mice by controlling for ApoA2 allelic effects: confirmation of a chromosome 6 locus in a congenic strain. *Physiol. Genomics*. **17**: 48–59.
50. Anunciado, R. V., M. Nishimura, M. Mori, A. Ishikawa, S. Tanaka, F. Horio, T. Ohno, and T. Namikawa. 2003. Quantitative trait locus analysis of serum insulin, triglyceride, total cholesterol and phospholipid levels in the (SM/J x A/J)F2 mice. *Exp. Anim.* **52**: 37–42.
51. Su, Z., A. Cox, Y. Shen, I. M. Stylianou, and B. Paigen. 2009. Farp2 and Stk25 are candidate genes for the HDL cholesterol locus on mouse chromosome 1. *Arterioscler. Thromb. Vasc. Biol.* **29**: 107–113.
52. Mehrabian, M., L. W. Castellani, P. Z. Wen, J. Wong, T. Rithaporn, S. Y. Hama, G. P. Hough, D. Johnson, J. J. Albers, G. A. Mottino, et al. 2000. Genetic control of HDL levels and composition in an interspecific mouse cross (CAST/Ei x C57BL/6J). *J. Lipid Res.* **41**: 1936–1946.
53. Maltais, L. J., J. A. Blake, T. Chu, C. M. Lutz, J. T. Eppig, and I. Jackson. 2002. Rules and guidelines for mouse gene, allele, and mutation nomenclature: a condensed version. *Genomics*. **79**: 471–474.